

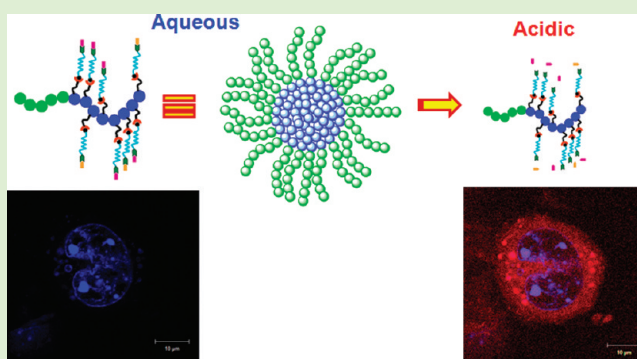
Norbornene Derived Doxorubicin Copolymers as Drug Carriers with pH Responsive Hydrazone Linker

Vijayakameswara Rao N,[†] Shivshankar R. Mane,[†] Abhinoy Kishore,[‡] Jayasri Das Sarma,^{*,‡} and Raja Shunmugam^{*,†}

[†]Polymer Research Centre, Department of Chemical Sciences and [‡]Department of Biological Sciences, Indian Institute of Science Education and Research Kolkata (IISER K), India

Supporting Information

ABSTRACT: The synthesis and complete characterization of both norbornene-derived doxorubicin (mono **1**) and polyethylene glycol (mono **2**) monomers are clearly described, and their copolymerization by ring-opening metathesis polymerization (ROMP) to get the block copolymer (COPY-DOX) is vividly elaborated. The careful design of these conjugates exhibits properties like well-shielded drug moieties and well-defined nanostructures; additionally, they show solubility in both water and biological medium and also have the important tendency of rendering acid-triggered drug release. The drug release profile suggests the importance of having the hydrazone linker that helps to release the drug exactly at the mild acidic conditions resembling the pH of the cancerous cells. It is also observed that the drug release from micelles of COPY-DOX is significantly accelerated at a mildly acidic pH of 5.5–6, compared to the physiological pH of 7.4, suggesting the pH-responsive feature of the drug delivery system with hydrazone linkages. Confocal laser scanning microscopy (CLSM) measurements indicate that these COPY-DOX micelles are easily internalized by living cells. MTT assays against HeLa and 4T1 cancer cells showing COPY-DOX micelles have a high anticancer efficacy. All of these results demonstrate that these polymeric micelles that self-assembled from COPY-DOX block copolymers have great scope in the world of medicine, and they also symbolize promising carriers for the pH-triggered intracellular delivery of hydrophobic anticancer drugs.



INTRODUCTION

Over the past two decades, several first-generation therapeutic molecular products have emerged in cancer therapy to galvanize the drug delivery system, which is a multidisciplinary scientific field undergoing explosive development.^{1a–c} Though they improved the therapeutic benefit of clinically validated cancer drugs by enhancing drug tolerability and efficacy, it is a great challenge for researchers in the field to generate an effective system that has enormous potential in providing controlled release and molecular targeting properties in these products.^{2a–c} The role of functionalized polymers has been widely investigated in this area of research, which has seen considerable growth during the above-mentioned periods.^{3a–c} There are several advantages that can be cited in favor of polymeric drugs over their monomeric precursors, like longer retention time in the body, lower toxicity, and a greater specificity of action.⁴ Recently, efforts have focused on developing drugs through self-assembly or high-throughput processes to facilitate the development and screening of them with these distinct properties.^{5a,b} But inherent characteristics of a conventional polymer synthesis, such as molecular weight distribution of a polymer sample, have induced enormous regulatory difficulties for the chosen synthetic strategy.⁶ We

have taken the initiative to overcome this factor by opting for a production technique like ROMP,^{7a–i} the living ring-opening metathesis polymerization, which is more attractive for the preparation of such monodisperse polymeric prodrugs due to the exceptional functional group tolerance of the Grubbs' catalyst employed in this process.^{8a–e}

Even though there are a lot of familiar methods and procedures that can be followed to control the release rate of drugs by covalently attaching them to a hydrolytically labile bond, such as an imine,⁹ acetal,¹⁰ oxime,^{11a–c} or orthoester,¹² we are very specific about hydrazone bonds for their responsive acuteness in delivery behavior and also for their usually facile incorporation of hydrazides into delivery materials.¹³ Typically, the release rate of the drug with hydrazone linkage is governed by the pH of the surrounding media, with faster release observed in acidic (pH 5–6) environments compared with physiological media (pH 7.4). However, incorporation of a hydrazone into polymer prodrugs is still synthetically challenging and not explored much except for very few

Received: October 20, 2011

Revised: November 20, 2011

Published: November 22, 2011

pioneering reports on poly(aspartate hydrazone adriamycin) based polymers.^{14a} A recent report shows the attachment of the doxorubicin moiety to methoxy poly(ethylene glycol)-*b*-poly-(lactide-*co*-2,2-dihydroxymethyl-propylene carbonate) by hydrazone linkage,^{14b} but it is done by the post-polymer modification chemistry. The drawback of post-functionalization here is that the control over attaching the drug to the polymer backbone could not be demonstrated precisely.

In this article, we report a simple and unique approach to the design and synthesis of the block copolymer (**COPY-DOX**) that has the potential application as a drug carrier. Motivated by the hydrolytically labile prospects of hydrazone bonds along with fascinating self-assembly properties of amphiphilic block copolymers, this work investigates the design and synthesis of the **COPY-DOX**, consisting of hydrazone-tethered DOX and PEG chains in the norbornene backbone. To avoid the unfavorable peripheral hydrophobicity,¹⁵ a well-shielded environment for the covalently attached DOX is achieved when it is copolymerized with poly(ethylene glycol) monomethyl ether (PEG) as another block. Also, the addition of PEG block makes the system advantageous, as it shows no toxicity and can significantly promote water-solubility and increase the plasma clearance half-life of nanostructures.¹⁶

EXPERIMENTAL SECTION

Materials: 5-norbornene-2-carboxylic acid (mixture of endo and exo isomers) and exo-oxabicyclo[2.2.1]hept-5-ene-2,3-dicarboxylic anhydride were prepared following the reported procedure. Doxorubicin hydrochloride, second generation Grubbs' catalyst, tertiary butyl carbazate, poly(ethylene glycol) monomethyl ether (PEG, $M_n = 700$ and 2000 g/mol), 4-aminobenzoic acid, acetic anhydride, sodium acetate, *N*-(3-dimethylaminopropyl)-*N'*-ethylcarbodiimide hydrochloride, *N*-hydroxysuccinimide, dicyclohexyl carbodiimide (DCC), 1-hydroxybenzotriazole, 4-dimethylamino-pyridine (DMAP), pyrene, $CDCl_3$, DMSO- d_6 , acetonitrile, dichloromethane, furan, maleic anhydride, toluene, vinyl ethyl ether, diethyl ether, methanol, dimethyl formamide (DMF), ethyl acetate, pentane, acetone, trifluoroacetic acid, and CD_3OD were purchased from Sigma Aldrich and used as received without further purification. Clear polystyrene tissue culture-treated 96-well and 6-well plates were obtained from Atlanta Drugs. Dimethyl sulfoxide (DMSO) was used after purification by distillation under vacuum and dried with calcium hydride (CaH_2). Tetrahydrofuran (THF) was refluxed over freshly prepared sodium benzophenone complex (a deep-purple color indicating an oxygen- and moisture-free solvent) and then distilled to use immediately. Anhydrous acetonitrile and dichloromethane were refluxed with CaH_2 and then distilled prior to use. All other reagents and solvents of analytical grade were used as received unless otherwise mentioned.

Cell Studies. Dulbecco's modified Eagle's medium (DMEM), minimal essential medium (MEM), penicillin, streptomycin, and fetal bovine serum (FBS) were purchased from Invitrogen. 3-(4,5-Dimethyl-2-thiazolyl)-2,5-diphenyl-2H-tetrazolium bromide (MTT) was purchased from USB (Cleveland, OH). Vectashield mounting medium with DAPI was obtained from Vector Laboratories.

Characterization. Gel Permeation Chromatography (GPC). Molecular weights and PDIs were measured by Waters gel permeation chromatography in THF relative to PMMA standards on systems equipped with Waters Model 515 HPLC pump and Waters Model 2414 Refractive Index Detector at 35 °C with a flow rate of 1 mL/min. HRMS analyses were performed with Q-TOF YA263 high resolution (Waters Corporation) instruments by +ve mode electrospray ionization.

Fluorometry. Fluorescence emission spectra were recorded on a fluorescence spectrometer (Horiba Jobin Yvon, Fluoromax-3, Xe-150 W, 250–900 nm).

Nuclear Magnetic Resonance (NMR). The 1H NMR spectroscopy was carried out on a Bruker 500 MHz spectrometer using $CDCl_3$ as a

solvent. 1H NMR spectra of solutions in $CDCl_3$ were calibrated to tetramethylsilane as internal standard (δ_H 0.00).

Fourier Transform Infrared (FT-IR). FT-IR spectra were obtained on FT-IR Perkin-Elmer spectrometer at a nominal resolution of 2 cm^{-1} .

Ultraviolet (UV) Spectroscopy. UV-visible absorption measurements were carried out on U-4100 spectrophotometer HITACHI UV-vis spectrometer, with a scan rate of 500 nm/min.

Dynamic Light Scattering (DLS). Particle size of QDs were measured by dynamic light scattering (DLS), using a Malvern Zetasizer Nano equipped with a 4.0 mW He-Ne laser operating at $\lambda = 633$ nm. All samples were measured in aqueous as well as methanol at room temperature and a scattering angle of 173°.

Transmission Electron Microscopy (TEM). Low resolution transmission electron microscopy (TEM) was performed on a JEOL 200 CX microscope. TEM grids were purchased from Ted Pella, Inc. and consisted of 3–4 nm amorphous carbon film supported on a 400-mesh copper grid.

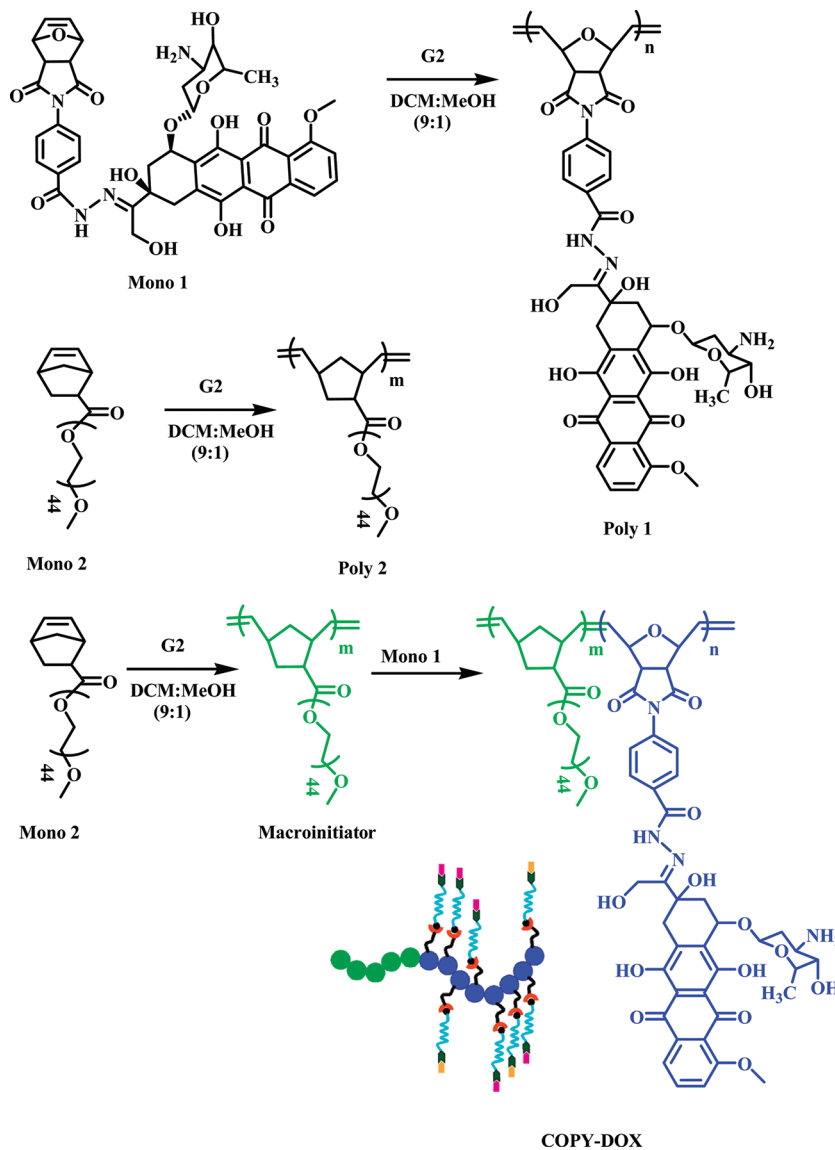
Confocal Laser Scanning Microscopy (CLSM). Confocal Microscope images were taken in LSM 710 with microscope axio observer Z.1, Carl Zeiss.

Synthesis of Norbornene-Derived Doxorubicin Hydrazone Linker (Mono 1). Doxorubicin hydrochloride, 29 mg (0.05 mmol), and compound 3, 72.6 mg (0.18 mmol), were dissolved in 10 mL of anhydrous methanol. Trifluoroacetic acid (3 μL) was added to the reaction mixture. The reaction mixture was stirred at room temperature for 24 h, while being protected from light. The reaction mixture was concentrated to a volume of 1 mL and added to acetonitrile (20 mL) dropwise with stirring. The resulting solution was allowed to stand at 4 °C. This product was isolated by centrifugation, washed with fresh methanol/acetonitrile (1:10), and dried under vacuum to yield the hydrazone linker of doxorubicin (15 mg, 51% yield). 1H NMR (DMSO- d_6 , 400 MHz): δ 11.8 (s, 1H), 7.69–7.95 (m, 7H), 7.79–7.80 (m, 2H), 6.62 (s, 2H), 5.43 (m, 2H), 5.26 (m, 2H), 5.30 (s, 2H), 4.95–4.97 (m, 1H), 4.85–4.88 (t, 1H), 4.56–4.57 (m, 1H), 4.17–4.18 (m, 1H), 4.21 (m, 1H), 4.02 (s, 3H), 3.55–3.56 (m, 1H), 3.11 (s, 2H), 2.95–3.02 (m, 2H), 2.13–2.15 (m, 2H), 1.88–1.89 (m, 1H), 1.6–1.69 (m, 1H), 1.16–1.19 (m, 3H). ^{13}C NMR (CD_3OD , 400 MHz): δ 215.0, 187.62, 188.82, 177.20, 162.77, 158.39, 156.46, 137.83, 129.04, 127.98, 122.16, 120.49, 112.12, 100.98, 82.81, 76.86, 71.78, 67.88, 61.0, 59.0, 39, 32.0, 33.81, 29.42, 16.98. IR (KBr, cm^{-1}): δ 3474, 2992, 2419, 1718, 1799, 1674, 1604, 1567, 1525, 1416, 1299, 114, 1258, 1154, 1026, 1006, 960, 900, 891, 788, 733. MS (ESI) calcd for $C_{28}H_{30}O_2Na$ [$M + H$]⁺, 824.25; observed, 824.9.

Synthesis of Norbornene Grafted Poly(ethyleneglycol) (Mono 2). Monomethoxy PEG, 100 mg (2.5 mmol), and 20 mg (2.9 mmol) of compound 4 were dissolved in 5 mL of dry dichloromethane. Dicyclohexyl carbodiimide, 597 mg (2.9 mmol), and a catalytic amount, 1.84 mg (10 mol %), of dimethyl amino pyridine were added to the mixture at room temperature. The reaction mixture was allowed to stir for 15 h. The resulting solid was removed by filtration and the filtrate was concentrated to a pasty mass. Dichloromethane/hexane (1:2) was charged to the pasty mass and kept overnight to obtain a solid (80 mg, 80% yield). 1H NMR ($CDCl_3$, 400 MHz): δ 6.0–6.1 (m, 2H), 3.80–4.2 (m, 4H), 3.3 (s, 2H), 3.0 (s, 1H), 2.9 (m, 1H), 2.19–2.28 (m, 2H), 1.2–1.6 (m, 2H). ^{13}C NMR ($CDCl_3$, 400 MHz): δ 176.0, 138.40, 135.63, 63.45, 61.58, 59.29, 46.19, 42.93, 41.48, 30.26, 26.39.

Homopolymerization of Mono 1. A total of 30 mg (0.0138 mmol) of mono 1 and second generation Grubbs' catalyst, 0.81 mg (15 mol %), were dissolved in a 3 mL solution of dry $CDCl_3$ and CD_3OD (9:1 v/v %) under nitrogen while being protected with light. The mixture was stirred at room temperature for 4 h. The resulting polymer was isolated by precipitating in cold ether and concentrated under vacuum. Gel permeation chromatography was done in tetrahydrofuran (flow rate = 1 mL/min). The molecular weight of the polymer was obtained using polystyrene standards ($M_n = 17400$; PDI = 1.17; 10 mg, 33% yield). 1H NMR (CD_3OD , 400 MHz): δ 7.94–7.9549 (m, 2H), 7.79–7.80 (m, 2H), 7.77–7.78 (m, 1H), 7.36–7.39 (m, 1H), 5.43 (m, 1H), 5.26 (m, 2H), 5.13–4.4.6 (m, 1H) 5.30 (s, 2H), 4.59 (d, 1H), 4.21 (m,

Scheme 1. Synthetic Methodology of COPY-DOX Block Copolymers



1H), 4.02 (s, 3H), 3.11 (s, 2H), 1.6–1.9 (m, 2H), 2.46 (m, 2H), 1.16–1.19 (m, 3H), 1.60–1.90 (m, 2H). IR (KBr, cm^{-1}): 3944, 3757, 3690, 3600, 3054, 2987, 2856, 2085, 2521, 2411, 2305, 2155, 2126, 2054, 1715, 1605, 1551, 1422, 1263, 1157, 1101, 1058, 1017, 896.

Homopolymerization of Mono 2. Mono 2, 100 mg (0.0408 mmol), and second generation Grubbs' catalyst, 0.346 mg (0.0004 mmol), were dissolved in dry dichloromethane (3 mL) under nitrogen, and the mixture was stirred at room temperature for 4 h. The resulting polymer was isolated by precipitating in cold ether and concentrated under vacuum. Gel permeation chromatography was done in tetrahydrofuran (flow rate = 1 mL/min). The molecular weight of the polymer was obtained using polystyrene standards. $M_n = 7000$, PDI = 1.04 (80 mg, 80% yield). $^1\text{H NMR}$ (CDCl_3 , 400 MHz): δ 5.0–5.3 (m, 2H new peaks were observed), 3.80–4.2 (PEG-H, 190H), 3.3 (s, 3H), 1.5–1.7 (m, 39H). IR (KBr, cm^{-1}): 3944, 3690, 3054, 2987, 2685, 2305, 1422, 1265, 1102, 896, 738, 706.

Synthesis of Block Copolymer (COPY-DOX). Known amounts of monomers 1 and 2 were weighed into two separate Schlenk flasks, placed under an atmosphere of nitrogen, and dissolved in anhydrous dichloromethane and methanol (9:1 v/v %). Into another Schlenk flask, a desired amount of third generation Grubbs' catalyst 0.63 mg (15 mol %) was added, flushed with nitrogen, and dissolved in a minimum amount of anhydrous dichloromethane and methanol (9:1 v/v %). All three flasks were degassed three times by freeze–pump–

thaw cycles. Monomer 2 (30 mg) was transferred to the flask containing the catalyst via a cannula. The reaction was allowed to stir at room temperature until the polymerization was complete (4 h), after which the second monomer 1 (12 mg) was added to the flask via a cannula. The polymerization was allowed to continue for another 24 h before it was quenched with ethyl vinyl ether (0.2 mL). An aliquot was taken for GPC analysis, and the remaining product was precipitated from pentane, dissolved again in THF, passed through neutral alumina to remove the catalyst, and precipitated again from pentane to get a pure COPY-DOX. Gel permeation chromatography was done in tetrahydrofuran (flow rate = 1 mL/min). The molecular weight of polymer using was measured using polystyrene standards. $M_n = 38000$, PDI = 1.05. $^1\text{H NMR}$ (CD_3OD , 400 MHz): δ 7.65–8.03 (s, q, d, d', e, e'), 5.17–5.47 (a, a', x, f, j, y), 4.20 (g'), 4.05 (n), 3.66 (z), 3.58–3.63 (k, w), 3.30 (n'), 3.0–3.03 (c, p', b), 2.10–2.19 (g), 1.60–1.90 (g', t, p, w, r), 1.29–1.32 (h). IR (KBr, cm^{-1}): 3944, 3757, 3690, 3601, 3054, 2987, 2930, 2685, 2521, 2411, 2305, 2155, 2127, 2055, 1968, 1737, 1605, 1550, 1422, 1265, 1155, 1107, 1017, 991, 896, 849.

Cell Culture. HeLa cells, a human uterine cervical cancer cell line, were maintained in Dulbecco's modified Eagle's medium (DMEM) with penicillin (100 U/mL) and streptomycin (100 $\mu\text{g}/\text{mL}$) plus 10% fetal bovine serum (FBS). Whereas, HEK-293, a human embryonic kidney cell line, was maintained in MEM containing 10% FBS (fetal bovine serum) with penicillin (100 U/mL) and streptomycin (100 $\mu\text{g}/$

mL) and 4T, a mouse mammary gland cancer cell line was maintained in RPMI containing 10% FBS (fetal bovine serum) with penicillin (100 U/mL) and streptomycin (100 µg/mL). All the cell lines were cultured for a month with 10 passages and maintained at 37 °C with 5% CO₂ in their respective medium.

Cellular Uptake Study. Confluent monolayers of HEK-293, HeLa, and 4T cells were seeded on 12 mm coverslips plated on 24-well tissue culture dishes in their respective medium. Confluent monolayer cells were treated with free Dox of COPY-DOX at different concentrations (1–20 µg) for 24 h. After 24 h post-treatment, cells were briefly washed in PBS with Ca²⁺ and Mg²⁺, fixed in a methanol/acetone (1:1) mixture for 2–5 min, successively washed with PBS without Ca²⁺ and Mg²⁺, and mounted in Vectashield with DAPI. The cellular uptake behavior and the intracellular distribution of free Dox and COPY-DOX were analyzed using confocal laser scanning microscope (Zeiss, LSM 710).

Cytotoxicity Assay of COPY-DOX. Cytotoxicity of COPY-DOX in HEK, HeLa, and 4T cell lines was quantitatively determined using MTT enzymatic and colorimetric assay. All cell lines were seeded at 1 × 10⁴ cells/well in 96-well plates and maintained in culture for 24 h at 37 °C in their respective medium. After 24 h, the medium was removed, cells were washed with PBS, and medium containing different concentrations of COPY-DOX (25–200 µg) was added to the designated wells. The whole experimental plate was incubated for 72 h. Fresh MTT (20 µL) from 5 mg/mL stock solution was added to each well, followed by incubation for 4 h at 37 °C. After 4 h, medium from the wells was removed and 100 µL of DMSO was added to each well and incubated for 15 min to completely solubilize the cells. The absorbance of the resulting solution was measured at 515 nm, and cell survivals were determined by comparison of optical density with untreated respective control cell cultures.

Cell-Growth Inhibition Assay by Trypan Blue Exclusion Method. Cells were seeded at 1.25 × 10⁴ cells in 24-well tissue culture plates and the inhibition activities of cell growth and division of Doxy polymer were quantitatively determined by visual cell counting using a hemocytometer chamber. After 24 h of cell plating, different concentrations of COPY-DOX (25–50 µg) was added to the respective wells. Designated wells for control were maintained with respective medium without adding any COPY-DOX. The whole plate was incubated for an additional 72 h. Cell counting was performed by the trypan blue exclusion method at 24, 48, and 72 h. The extent of cell inhibition was determined by viable cell population counts and compared with untreated control cell culture for each time point.

RESULTS AND DISCUSSION

Monomer Synthesis (Scheme 1). Exo-5-norbornene-2-carboxylic acid was separated from the commercially available mixture of endo- and exo-5-norbornene-2-carboxylic acid by the idolactization methods of Ver Nooy and Rondstedt (see Supporting Information (SI)). From the ¹H NMR, the carboxylic acid signal was observed at δ 12 ppm (br, 1H; Figure S7). The signals at δ 6.02–6.06 ppm (m, 2H) correspond to norbornene olefinic protons, while the signals at δ 1.97–2.05 ppm (dt, *J* = 12.7 Hz, 1H) and δ 1.66–1.71 (m, 1H) belong to norbornene-bridged hydrogens. It was further confirmed by FT-IR (Figure S12) where the stretching mode due to carboxylic acid of exo-norbornene carboxylic acid was observed at 1700 cm⁻¹. Norbornene-grafted poly(ethyleneglycol) was prepared by coupling reaction between carboxylic acid and alcohol derivative of monomethoxy PEG using dicyclohexyl carbodiimide (DCC) and 4-dimethylaminopyridine (DMAP). Formation of the monomer was confirmed by ¹H NMR and FT-IR spectroscopies. In the product, ¹H NMR carboxylic acid signals at 12 ppm were absent, which was evident that exo-norbornene carboxylic acid was completely reacted with alcohol derivative of monomethoxy PEG. The signals at δ 3.65–4.3 ppm were due to the PEG (H-PEG),

while the signal at δ 3.37 (3H) was responsible for methyl group of poly(ethylene glycol) methyl ether (Figure 1a). The

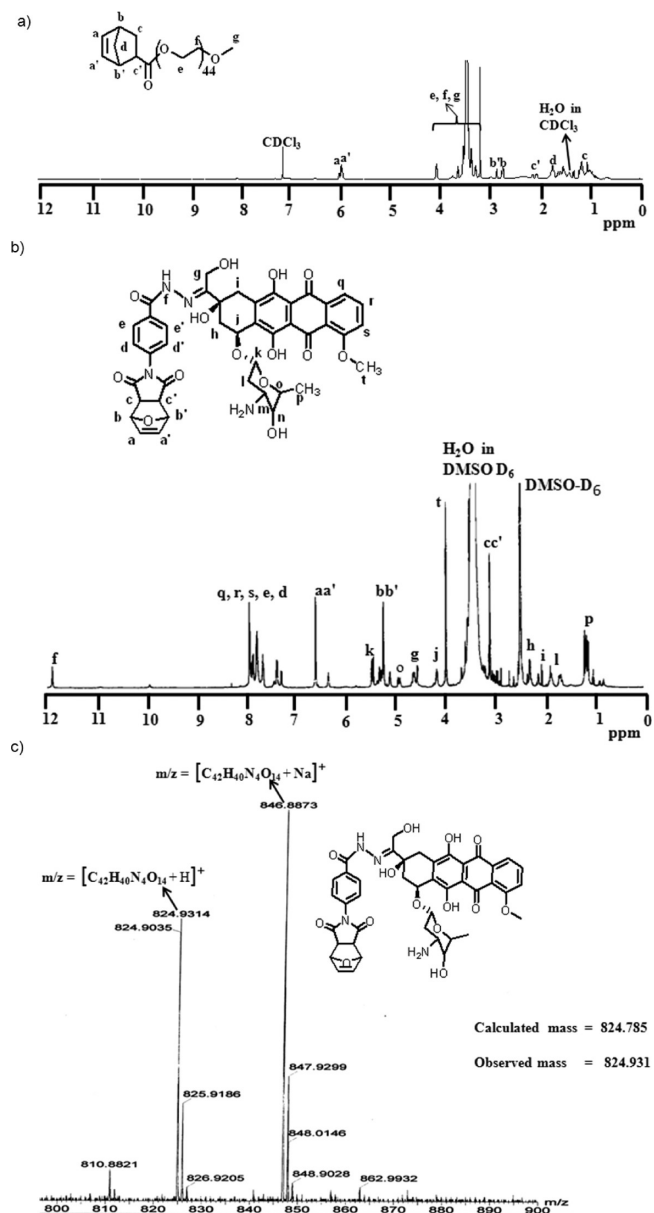


Figure 1. (a) ¹H NMR spectrum of mono 2; (b) ¹H NMR spectrum of mono 1; (c) mass spectrum of mono 1.

signals at δ 1.5 ppm (d, 1H) and δ 1.75 ppm (d, 1H) were for norbornene-bridged protons. The signals at δ 6.0–6.4 ppm (m, 2H) correspond to norbornene olefinic protons.

Exo-oxabicyclo[2.2.1]hept-5-ene-2,3-dicarboxylic anhydride was prepared following the reported process.¹³ 3-(4-Carboxyphenylcarbamoyl)-7-oxabicyclo[2.2.1]hept-5-ene-2-carboxylic acid was prepared by using 1 equiv of 4-aminobenzoic acid and 5.1 equiv of acetic anhydride in the presence of 0.29 equiv of sodium acetate in dimethyl formamide solvent. Product was confirmed by ¹H NMR and FT-IR spectroscopy. The signal at δ 13.1 (bs, 1H) ppm was responsible for carboxylic acid group (Figure S1) while signals at δ 8.0–8.2 (m, 2H) and 7.4–7.5 (m, 2H) ppm were responsible for aromatic protons. The specific signals at δ 6.6 (s, 2H), 5.34 (s, 2H), and 3.1 (s, 2H) ppm peaks were for oxo-norbornene protons. Broad stretching frequency

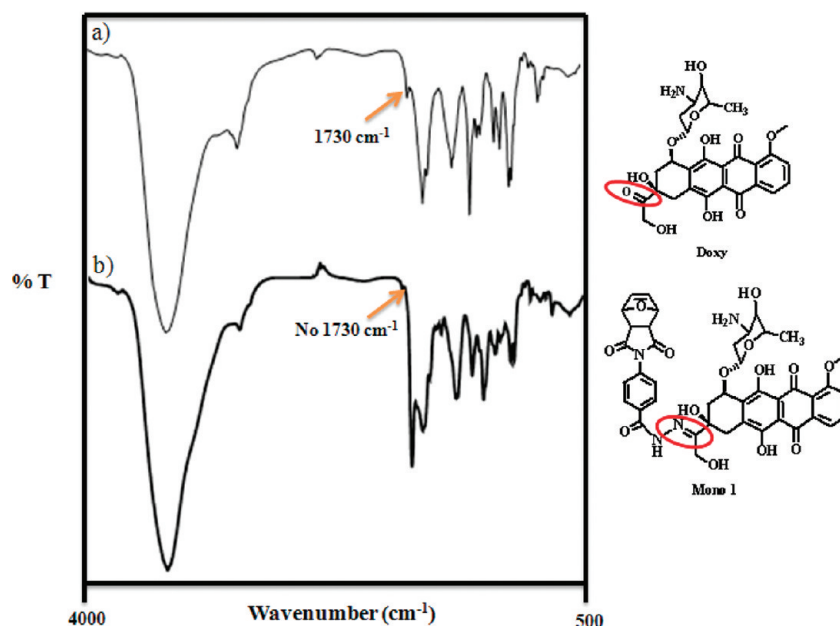


Figure 2. FT-IR spectra of (a) free doxorubicin and (b) mono **1**.

from FT-IR spectroscopy at 3244 cm^{-1} was attributed to free carboxylic acid as shown in (Figure S11a).

Tertiary butyl hydrazone nadic carboxylate was prepared by coupling of nadic acid and tertiary butyl carbazate using 1.2 equiv of *N*-(3-dimethylaminopropyl)-*N'*-ethylcarbodiimide hydrochloride (EDC) coupling reagent in the presence of 1.2 equiv of 1-hydroxybenzotriazole (HOBT) in dimethyl formamide solvent. Formation of the product was confirmed by ^1H NMR and FT-IR spectroscopy. The proton signal at δ 1.26 (s, 9H) ppm was responsible for the tertiary butyl group, while signals at δ 10.30 (bs, 1H) and δ 8.96 (s, 1H) were for hydrazone protons. The signals at δ 7.8–7.9 (m, 2H) and δ 7.2–7.26 (m, 2H) were for the benzene ring protons. The signals at δ 6.60 (s, 2H), 5.34 (s, 2H), and δ 3.11 (s, 2H) ppm were observed for oxo-norbornene protons (Figure S3). The stretching frequency at 3244 cm^{-1} for free carboxylic acid was shifted to 3277 cm^{-1} , which indicated the formation of amide group as shown (Figure S11b). In the next step, *tert*-butoxy carbonyl group was cleaved using trifluoroacetic acid to yield the hydrazide. This product was confirmed by ^1H NMR and FT-IR spectroscopy. The signal at δ 1.26 (s, 9H) ppm for tertiary butyl group was absent in the product, which indicated the complete deprotection of tertiary butyl group (Figure S5). Shifting of stretching frequency from 3277 to 3473 cm^{-1} indicated the formation of the free amine group (Figure S11c).

Doxorubicin with hydrazone linker (mono **1**) was prepared by addition of doxorubicin hydrochloride and norborne hydrazide in methanol in presence of trifluoroacetic acid and the whole reaction set up was protected from light for 24 h. The product was confirmed by ^1H NMR and IR spectroscopy. The signals at δ 7.94–7.95 (m, 2H), 7.79–7.80 (m, 2H), 7.77–7.78 (m, 1H), and 7.36–7.39 (m, 1H) ppm were responsible for doxorubicin aromatic group protons. The signal at δ 6.62 (s, 2H) was observed for the norbornene olefinic protons (Figure 1b). In mono **1**, the band at 1730 cm^{-1} , which was responsible for carbonyl stretching frequency of free doxorubicin was absent and that indicated the formation of hydrazone linker between ketone and hydrazine (Figure 2a,b). All the monomers were characterized by micromass spectrometer (Q-TOF), using

methanol as solvent. Observed mass (m/z) and calculated mass for all monomers were in good agreement, which confirmed the formation of product.

Polymerization Reactions. Homopolymerization.

Homopolymerization of mono **1** was carried out by using second generation Grubbs' catalyst at room temperature in dry CDCl_3 and CD_3OD (9:1 v/v %) solvent system and monitored by ^1H NMR. New signals were observed at δ 5–5.3 ppm, and norbornene olefinic protons disappeared at δ 6.6 ppm, indicating the formation of the product. Molecular weight of the polymer, poly **1**, was determined by the gel permeation chromatography, as shown in Figure S13 ($M_n = 17400$ with PDI 1.17). The stretching frequency at 1567 cm^{-1} for norbornene olefinic bond (C=C) was absent, which confirmed the formation of homopolymer (Figure S14). The poly **2** was prepared by using second generation Grubbs' catalyst ($M/I = 15$) at room temperature in DCM. Within 1 h, new peaks were observed at δ 5.0–5.3 ppm, and norbornene olefinic protons were disappeared at δ 6.0–6.1 ppm, as shown in Figure S10. The stretching frequency at 1567 cm^{-1} for the norbornene olefinic bond (C=C) was absent, which confirmed the formation of poly **2** (Figure S15).

Block Copolymerization. Known amounts of monomers (mono **1** and **2**) were weighed into two separate Schlenk flasks, placed under an atmosphere of nitrogen, and dissolved in anhydrous dichloromethane and methanol (9:1 v/v %). Into another Schlenk flask, a desired amount of second generation Grubbs' catalyst was added, flushed with nitrogen, and dissolved in minimum amount of anhydrous dichloromethane and methanol (9:1 v/v %). All three flasks were degassed three times by freeze–pump–thaw cycles. The reaction mixture was stirred at room temperature for 4 h. Then monomer **1** was added to the reaction mixture and stirred at room temperature for 24 h. The whole reaction was monitored by ^1H NMR for every 1 h. New peaks were observed at 5.0–5.3 ppm, and norbornene olefinic protons disappeared at 6.6 ppm, indicating the formation of the product. The stretching frequency at 1567 cm^{-1} for the norbornene olefinic (C=C) bond was absent in COPY-DOX (Figure S16), which confirmed the polymer

formation. The reaction mixture was quenched with ethyl vinyl ether (0.2 mL). An aliquot was taken for GPC analysis, and the remaining product was precipitated from pentane, dissolved again in THF, passed through neutral alumina to remove the catalyst, and precipitated again from pentane to get a pure **COPY-DOX**. Molecular weight of the polymer was characterized by THF-GPC, which showed $M_n = 38000$ with PDI 1.05 value (Figure 3b). It was observed from the GPC that all

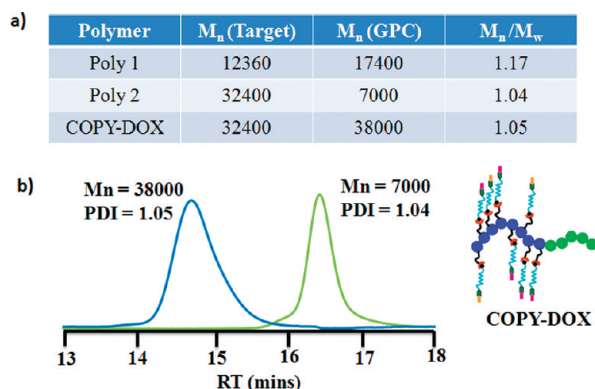


Figure 3. (a) Table comprising molecular weight and PDI of poly 1 and 2 and **COPY-DOX**; (b) gel permeation chromatogram of **COPY-DOX** confirms the formation of block copolymer. It was calculated that 1 mg of **COPY-DOX** ($M_n = 38000$) contains 2.631×10^{-6} mol % of doxorubicin.

the macroinitiator was completely converted to the block copolymer (Figure 3b) with very narrow PDI. All the polymerization showed the controlled behavior and produced monodisperse polymers (Figure 3a).

Determination of Critical Micelle Concentration of COPY-DOX. Critical micelle concentration (CMC) was measured by using pyrene as an extrinsic probe.¹⁷ Pyrene (4 μg) was dissolved in methanol. Several samples were prepared with different concentration of **COPY-DOX**. The **COPY-DOX** was dissolved in 1000 μL of methanol and 5 mL of water was added to the samples. The solution was stirred at room temperature to evaporate the organic solvent. The fluorescence intensities of prepared solutions were measured by spectrofluorometer. The concentration of pyrene was maintained at 0.2 μM and final concentration of **COPY-DOX** was changed from 0.01 to 1 $\mu\text{g}/\text{mL}$, with the excitation wavelength set at 339 nm; the emission intensities were determined at 371, 382, and 396 nm. The relative emission fluorescence intensities of 396/371 nm was varied as a function of **COPY-DOX** concentration (Figure 4a). The CMC was determined by taking copolymer concentration value at which the relative fluorescence intensity ratio began to change. The observed CMC was 0.923 $\mu\text{g}/\text{mL}$.

Morphology of COPY-DOX Micelles. A total of 1 mg of block copolymer (**COPY-DOX**) was dissolved in 10 mL of methanol and stirred for 1 h to ensure the complete polymer solubilization. From this solution, 2.5 mL of sample was taken in a vial to which 18% of water was added under constant stirring. Dynamic light scattering (DLS) analysis was performed on the solution and the particle size was measured (Figure 4b). The size of the micelles was about 105 nm with 0.25 PDI. The morphology of the micelles was determined by AFM (Figure 4c) as well as TEM (Figure 4d). From TEM and AFM analysis, the particle size was also measured to be about 100 nm, which was in good agreement with DLS measurements (Figure 4b). It

was also observed from AFM and TEM that the observed micelles from **COPY-DOX** were spherical in shape and assembled in controlled manner.

In Vitro Doxorubicin (DOX) Release. Dialysis Study.

For the drug release profile of **COPY-DOX**, pH 7.4 as well as acidic conditions were studied, as the normal pH of blood for sustaining human life is about 7.4, while the endosomes and lysosomes of cells have a more acidic environment.^{11c} Therefore, the drug release study of **COPY-DOX** micelles was carried out in pH 7.4 in phosphate buffer solution and pH 5.5 and 6 in acetate buffer solutions, respectively.¹⁸ A total of 1 mg of block copolymer (**COPY-DOX**) was dissolved in 1 mL of distilled water and loaded in a dialysis tube (3500; Dalton cutoff) and dialyzed against 70 mL of a buffer solution whose pH was maintained at 5.5. An aliquot of the sample was removed and its absorbance at 480 nm was measured as an indication of the release of doxorubicin. Fluorescence also recorded by exciting the solution at 510 nm. Emissions from the free DOX released from **COPY-DOX** were observed at 560 and 590 nm. The sample was then added back to the solution to maintain the volume of the solution. This procedure was repeated for every 1 h and results were observed for 48 h. It was observed that, after 24 h, there was no significance increase in the intensity of fluorescence and UV intensity (Figure 5a). The similar procedure was repeated to monitor the drug release at pH 6.0 (Figure 5b), as well as pH 7.4, and the results are shown in Figure 5c. The DOX release from **COPY-DOX** at pH 7.4 was very minimal (less than 5%), which was very interesting to observe, as it clearly demonstrated the **COPY-DOX** micelle's stability in the physiological condition. It was also very worthy to note that the maximum as well as fast release was observed at pH 5.5 compared to pH 6 or 7.4, which suggested the importance of having the acid-labile hydrazone linker in the **COPY-DOX**.

To Investigate the Ability of the COPY-DOX To Affect the In Vitro Efficacy. Slow release of Dox, through acid-labile linkages, inside acidic cancerous cells and endosomes should give our **COPY-DOX** with pH linker additional selective edge over the free drug. To study the in vitro efficacy of the release of **COPY-DOX** with pH linker three different cell lines were chosen such as human embryonic kidney cell line (HEK-293) and two cancerous cell lines: a human uterine cervical cancer cell line (Hela cells) and a mouse mammary gland cancer cell line (4T). Three different cell lines were grown in culture with similar kinetics and the pH of the cell medium.

Uptake of **COPY-DOX** in all the cells was through endocytosis and occurred relatively slowly inside the cell compared to free DOX. The uptake of free DOX occurred in about 6–8 h in all the cell lines, which could be clearly visible by fluorescent microscope after 12 h of post treatment (data not shown). Interestingly, the uptake of **COPY-DOX** appeared to be different. Post treatment of **COPY-DOX** at 24 h did not show any intracellular accumulation in the HEK-293 cells, but a diffused intracellular accumulation was observed in Hela cells and 4T cells. There was a clear endosomal/lysosomal **COPY-DOX** penetration that was observed (Figure 6).

The pH of the medium was relatively low in 4T cells in culture compared to HEK-293 and Hela, consecutively the release of DOX from **COPY-DOX** was more pronounced in 4T cells compare to Hela and HEK-293. The known acidic environment formed during endosomal uptake process, would induce DOX release from the **COPY-DOX** in 4T and Hela cells compared to HEK-293. Increasing the incubation time did

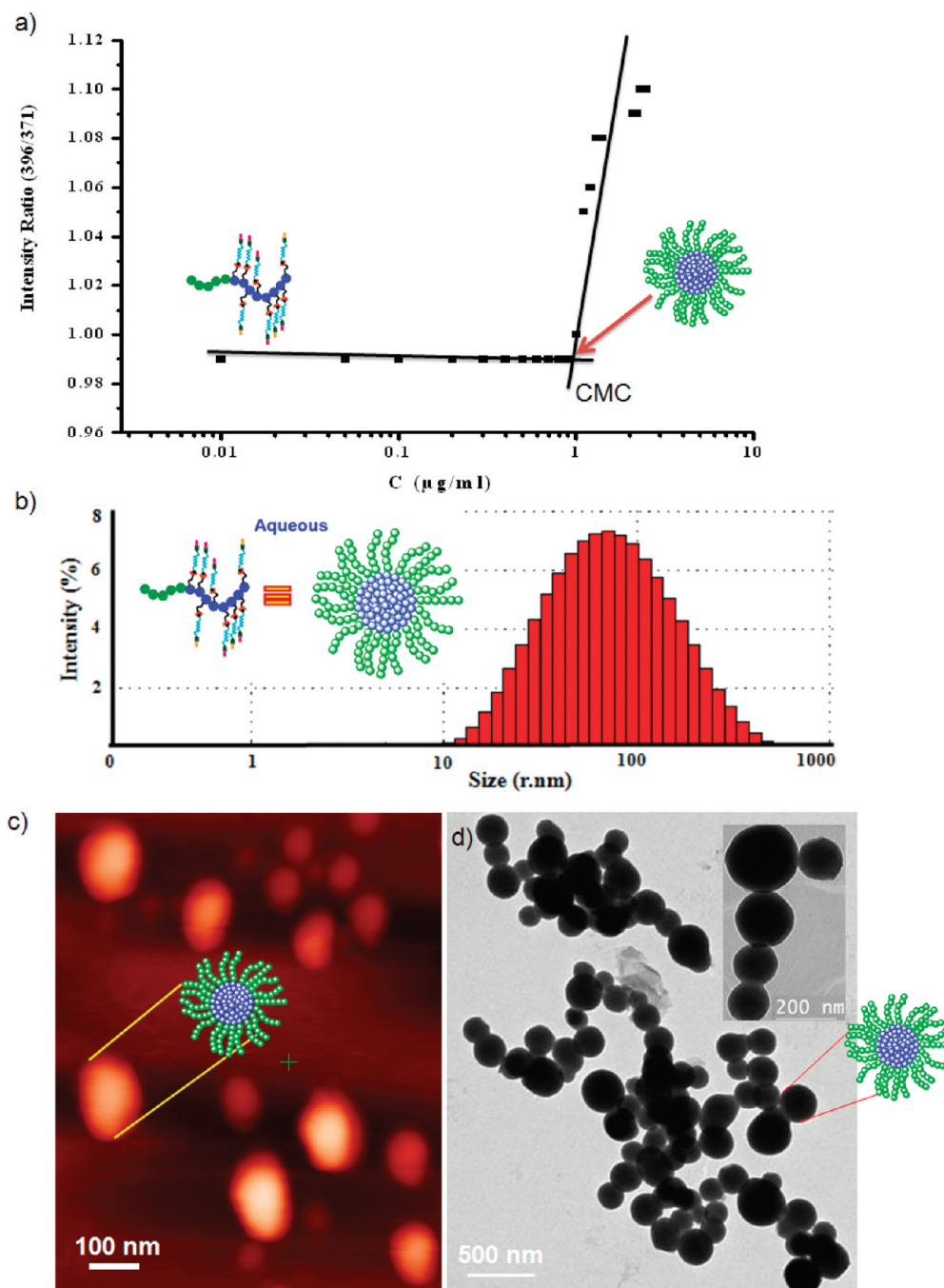


Figure 4. (a) Plot of concentration of COPY-DOX vs intensity ratio of emissions at 375 and 396 nm from pyrene. The observed CMC was 0.923 $\mu\text{g/mL}$. (b) DLS measurement of COPY-DOX micelles in aqueous solution. The size of the micelles was about 105 nm with 0.25 PDI. (c) Representative AFM image of COPY-DOX micelles spin-coated on a silicon surface. (d) TEM images of COPY-DOX micelles dip-casted on carbon-coated copper grids. The inset shows the proposed self-assembled structure of COPY-DOX block copolymers in an aqueous environment.

not change the rate or amount of internalization (data not shown). Mean intensity of fluorescence (released DOX) was plotted from 10 frames for each concentration (Figure 6) and it was noted that the amount of release of Dox from the COPY-DOX was highest in 4T compare to that followed by Hela compared to HEK-293. It was a very interesting observation to note as it emphasized the importance of our design of COPY-DOX with the hydrazone linker that released more Dox in 4T because 4T cells are more acidic than Hela cells.

The effect of COPY-DOX on the cell viability was evaluated by incubating COPY-DOX with increasing concentration (25

to 200 μg) for 72 h, at which time the viability of the cells was determined by MTT assay. HEK-293 cells showed significant cytotoxic effect at relatively higher concentration (200 μg), whereas Hela cells showed significant cytotoxic effect from the concentration of 100 μg , but 4T cells were more susceptible for COPY-DOX, and the significant effect of cytotoxicity was observed as low as 25 $\mu\text{g/mL}$ concentration. Interestingly, at higher concentration (100–200 μg), all three cells lines were showing cytotoxicity, which suggested that there was an imperfect uptake of nanoparticles into the cells above the threshold, as shown in Figure 7. The observed cytotoxicity could

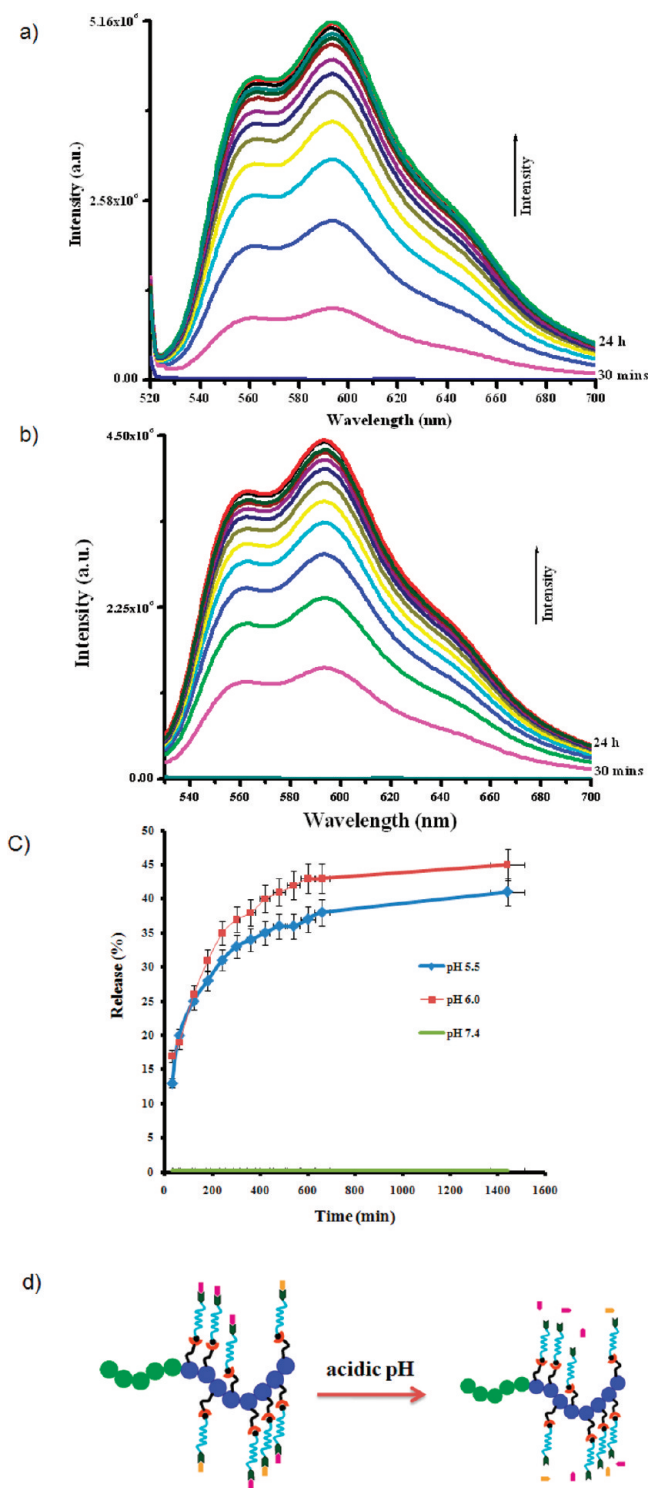


Figure 5. Drug release studies of COPY-DOX polymer. Fluorescence response was measured with varying time intervals at (a) pH 5.5; (b) pH 6; (c) DOX release profile from COPY-DOX micelles at 37 °C in comparison with pH 5.5, 6, and 7.4; (d) A cartoon representation of breaking of the hydrazone linkage at acidic pH and releasing the drug.

be attributed to the damage to cytoplasmic, endosomal, and lysosomal membranes, which could lead to cell death. Internalization and release of DOX-induced cytotoxicity could have a profound effect on cell growth and cell division.

The effect of COPY-DOX on cell growth and cell division was observed by incubating the nanoparticle in all three cell

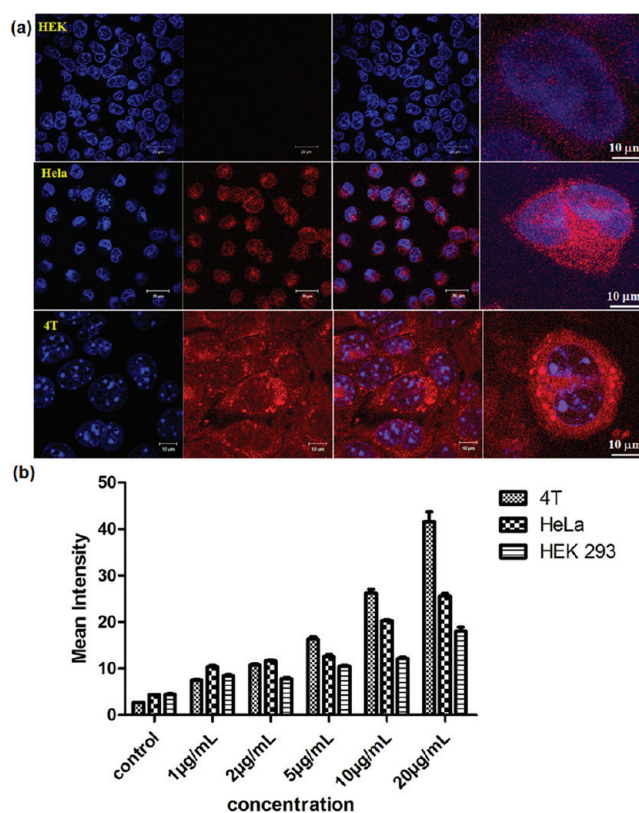


Figure 6. (a) Uptake of Doxy block copolymer in HEK-293, HeLa, and 4T cells. Cells were plated on coverslips inserted into the wells of 24-well tissue culture plates. Confluent monolayer cells were loaded with Dox and COPY-DOX at different concentrations (1–20 µg) for 24 h. Uptake studies were performed at 24 h post loading of Doxy and were analyzed using confocal laser scanning microscope (LSM 710; Carl Zeiss). Mean intensity fluorescence as an index of release of Dox from COPY-DOX after 24 h of incubation at different concentrations were plotted. Ten different frames were acquired from each concentration of treatment in a LSM 710 confocal microscope. Area of each frame was 45176.68 µm². Mean intensities were calculated for each frame and the mean of mean intensity was plotted against the concentration. Ten frames were taken from the each concentration at 40× in a LSM710 Zeiss confocal microscope.

lines. Significant cell growth inhibition was observed in both HeLa cells and 4T, whereas no significant cell growth inhibition was observed in HEK-293 cells at a concentration range of 25–50 µg (Figure 7).

CONCLUSION

This paper describes a novel approach by which a polymeric micelle exhibits well-shielded drug moieties, significant water, as well as biological medium, solubility, well-defined nanostructures, and acid-triggered drug release to elevate the efficacy and safety of the loaded drugs. To prepare such micelles, amphiphilic COPY-DOX block copolymer that has shell-forming PEG block along with core-forming DOX functionality conjugated through acid-sensitive hydrazone bonds to the side chains of the norbornene block are synthesized. To our knowledge, this report represents the simplest route to produce block copolymers containing a narrow polydispersity and a high density of drugs that are delivered efficiently in the acidic environment (pH 5–6). This newly designed block copolymer self-assembled into a spherical nanostructure in aqueous solutions that is confirmed by DLS, AFM, and TEM analysis.

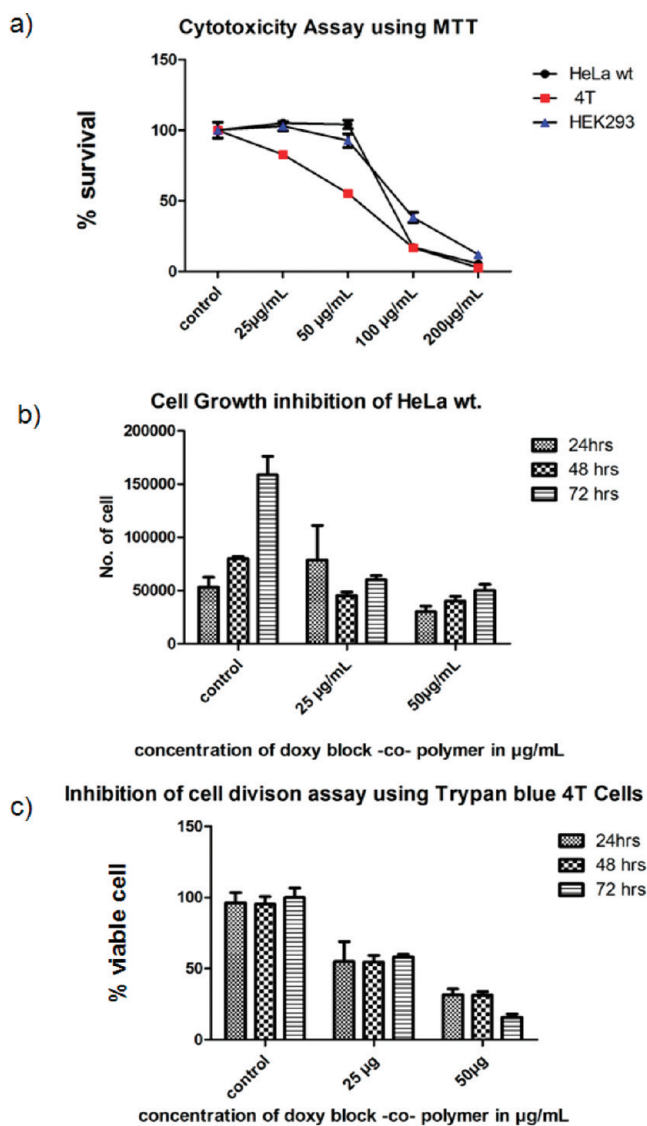


Figure 7. (a) Cytotoxicity profile of COPY-DOX block copolymer in HEK-293, HeLa, and 4T cells. HEK-293, HeLa, and 4T cells were seeded at 1×10^4 cells/well in 96-well plates, maintained in their respective medium, and treated with different doses of Doxy (25–200 µg). Data on the cytotoxicity level of COPY-DOX in each cell line was determined by MTT assay and after 72 h of post-treatment. (b) Effect of COPY-DOX block copolymer on cell growth was determined by the trypan blue exclusion method. The effect of cell viability was determined in HeLa cells by incubating each cell line with either 25 or 50 µg of Doxy block copolymer for 72 h and counting viable cells at 24, 48, and 72 h time intervals by visual cell counting using a hemocytometer. (c) 4T cell trypan blue exclusion methods.

Observed experimental results demonstrates that this micelle, with pH sensitivity, has a capacity to not only selectively control intracellular environment-sensitive drug release, but also to significantly enhance drug delivery efficiency by affecting drug efficacy with short exposure times. In vitro cytotoxicity assay and confocal microscopy analysis clearly indicated that cell growth inhibitory activity of the micelle was enhanced due to enhanced cellular uptake. Conclusively it can be proclaimed that the new polymeric micelle with the hydrazone linker denotes a technical nanoassembly showing excellent performance inside the cell as an efficient drug delivery system. Moreover, the system also promises an effective strategy and

new modalities for the creation of cancer therapy with macromolecular drug carrier to interact with living organisms. Future work in this area by our group will concentrate on improving the targeted delivery by incorporating folate functionality to COPY-DOX micelles not only to selectively control intracellular environment-sensitive drug release, but also to significantly enhance drug delivery efficiency by affecting drug efficacy with short exposure times.

■ ASSOCIATED CONTENT

Supporting Information

Additional analytical data, synthetic scheme, procedures, and references. This material is available free of charge via the Internet at <http://pubs.acs.org>.

■ ACKNOWLEDGMENTS

R.N.V., S.R.M., and A.K. thank IISER-Kolkata for the research fellowship and R.S. thanks DST, New Delhi, for Ramanujan Fellowship. R.S. and J.D.S. thank IISER-Kolkata for the infrastructure and start up funding. Authors also thank Mr. Ritabrata Ghosh for his assistance with confocal measurement.

■ REFERENCES

- (1) (a) Duncan, R. *Nat. Rev. Cancer* **2006**, *6* (9), 688–701. (b) Duncan, R. *Nat. Rev. Drug Discovery* **2003**, *2* (5), 347–360. (c) Duncan, R.; Kopecek, J. *Nat. Rev.* **1984**, *57*, 51–101.
- (2) (a) Helminger, G.; Sckell, A.; Dellian, M.; Forbes, N. S.; Jain, R. K. *Clin. Cancer Res.* **2002**, *8*, 1284–1291. (b) Duncan, R. *Anti-Cancer Drugs* **1992**, *3*, 175–210. (c) Duncan, R. *Biochem. Soc. Trans.* **2007**, *35* (1), 56–60.
- (3) (a) Singla, A. K.; Garg, A.; Aggarwal, D. *Int. J. Pharm.* **2002**, *235*, 179–192. (b) Stukel, J. M.; Li, R. C.; Maynard, H. D.; Caplan, M. R. *Biomacromolecules* **2010**, *11*, 160–167. (c) Christman, K. L.; Broyer, R. M.; Schopf, E.; Kolodziej, C. M.; Chen, Y.; Maynard, H. D. *Langmuir* **2011**, *27* (4), 1415–1418.
- (4) Maeda, H.; Wu, J.; Sawa, T.; Matsumura, Y.; Hori, K. *J. Controlled Release* **2000**, *65*, 271–284.
- (5) (a) Ghosh, S.; Basu, S.; Thayumanavan, S. *Macromolecules* **2006**, *39*, 5595–5597. (b) Satav, S. S.; Bhat, S.; Thayumanavan, S. *Biomacromolecules* **2010**, *11*, 1735–1740.
- (6) Maisie, J.; Samantha, M.; Todd, E. *Chem. Commun.* **2010**, *46*, 1377–1393.
- (7) (a) Grubbs, R. H. *Handbook of Metathesis*; Wiley-VCH: New York, 2003; Vol. 3. (b) Watson, K. J.; Park, S.-J.; Im, J.-H.; Nguyen, S. T. *Macromolecules* **2001**, *34*, 3507. (c) Mortell, K. H.; Gingras, M.; Kiessling, L. L. *J. Am. Chem. Soc.* **1994**, *116*, 12053. (d) Maynard, H. D.; Sheldon, Y. O.; Grubbs, R. H. *Macromolecules* **2000**, *33*, 6239. (e) Pollino, J. M.; Stubbs, L. P.; Weck, M. *Macromolecules* **2003**, *36*, 2230. (f) Schubert, U. S.; Eschbaumer, C. *Angew. Chem., Int. Ed.* **2002**, *41*, 2892. (g) Meyer, E.; Castellano, R. K.; Diederich, F. *Angew. Chem., Int. Ed.* **2003**, *42*, 1210. (h) Bergbreiter, D. E. *Angew. Chem., Int. Ed.* **1993**, *38*, 2870. (i) Young, J. W.; Sharpless, K. B. *Org. Chem.* **1988**, *1*, 240–242.
- (8) (a) Bertin, P. A.; Watson, K. J.; Nguyen, S. T. *Macromolecules* **2004**, *37*, 8364–8372. (b) Bertin, P. A.; Smith, D.; Nguyen, S. T. *Chem. Commun.* **2005**, 3793–3795. (c) Colak, S.; Nelson, C. F.; Nusslein, K.; Tew, G. N. *Biomacromolecules* **2009**, *10* (2), 353–359. (d) Lienkamp, K.; Tew, G. N. *Chem.—Eur. J.* **2009**, *15*, 11784–11800. (e) Madkour, A. E.; Koch, A. H. R.; Lienkamp, K.; Tew, G. N. *Macromolecules* **2010**, *43*, 4557–4561.
- (9) Gillies, E. R.; Frechet, J. M. J. *Bioconjugate Chem.* **2005**, *16*, 361–368.
- (10) Gillies, E. R.; Frechet, J. M. J. *Chem. Commun.* **2003**, *14*, 1640–1641.
- (11) (a) Lehn, J.-M.; Eliseev, A. *Science* **2001**, *291*, 2331–2332. (b) Lehn, J.-M. *Chem. Soc. Rev.* **2007**, *36*, 151–160. (c) Jin, Y.; Song,

L.; Su, Y.; Zhu, L.; Pang, Y.; Qiu, F.; Tong, G.; Yan, D.; Zhu, B.; Zhu, X. *Biomacromolecules* **2011**, *12*, 3460–3468.

(12) Gillies, E. R.; Frechet, J. M. J. *Pure Appl. Chem.* **2004**, *76*, 1295–1307.

(13) Matson, J. B.; Stupp, S. I. *Chem. Commun.* **2011**, *47* (28), 7962–7964.

(14) (a) Bae, Y.; Fukushima, S.; Harada, A.; Kataoka, K. *Angew. Chem., Int. Ed.* **2003**, *42*, 4640–4643. (b) Xiuli, H.; Shi, L.; Yubin, H.; Xuesi, C.; Xiabin, J. *Biomacromolecules* **2010**, *11*, 2094–2102.

(15) Tong, R.; Cheng, J. *Polym. Rev.* **2007**, *47*, 345–381.

(16) Gref, R.; Minamitake, Y.; Peracchia, M. T.; Trubetskoy, V.; Torchilin, V.; Langer, R. *Science* **1994**, *263*, 1600–1603.

(17) Hyuk, S. Y.; Lee, E. H.; Park, T. G. *J. Controlled Release* **2002**, *82*, 17–27.

(18) Hruby, M.; Konak, C.; Ulbrich, K. *J. Controlled Release* **2005**, *103*, 137–148.